

# Lensing and Waveguiding of Ultraslow Pulses in an Atomic Bose-Einstein Condensate

Devrim Tarhan<sup>\*,a</sup>, Alphan Sennaroglu<sup>b</sup>, Özgür E. Müstecaplıoğlu<sup>b,c</sup>

<sup>a</sup>*Department of Physics, Harran University, Osmanbey Yerleşkesi, Şanlıurfa, 63300, Turkey*

<sup>b</sup>*Department of Physics, Koç University, Rumelifeneri yolu, Sarıyer, Istanbul, 34450, Turkey*

<sup>c</sup>*Institute of Quantum Electronics, ETH Zurich Wolfgang-Pauli-Strasse 16, CH-8093 Zurich, Switzerland*

---

## Abstract

We investigate lensing and waveguiding properties of an atomic Bose-Einstein condensate for ultraslow pulse generated by electromagnetically induced transparency method. We show that a significant time delay can be controllably introduced between the lensed and guided components of the ultraslow pulse. In addition, we present how the number of guided modes supported by the condensate and the focal length can be controlled by the trap parameters or temperature.

*Key words:*

Bose-Einstein condensate, Electromagnetically induced transparency, ultraslow pulse propagation, Waveguides, Lenses

*PACS:* 03.75.Nt, 42.50.Gy, 41.20.Jb, 42.82.Et, 42.79.Bh

---

---

\*Corresponding author. Address: Department of Physics, Harran University, Osmanbey Yerleşkesi, Şanlıurfa, 63300, Turkey. Tel.: +90 414 3183578; fax: +90 414 3440051.

*Email address:* dtarhan@harran.edu.tr (Devrim Tarhan)

## 1. Introduction

Quantum interference effects, such as electromagnetically induced transparency (EIT) [1, 2], can produce considerable changes in the optical properties of matter and have been utilized to demonstrate ultraslow light propagation through an atomic Bose-Einstein condensate (BEC) [3]. This has promised a variety of new and appealing applications in coherent optical information storage as well as in quantum information processing . However, the potential of information storage in such systems is shadowed by their inherently low data rates. To overcome this challenge, exploitation of transverse directions for a multimode optical memory via three dimensional waveguiding of slow EIT pulse [4] has been recently suggested for BECs [5]. Transverse confinement of slow light is also quintessential for various proposals of high performance intracavity and nanofiber slow light schemes (See e.g. Ref. [6] and references therein). Furthermore, temperature dependence of group velocity of ultraslow light in a cold gas has been investigated for an interacting Bose gases [7].

A recent experiment, on the other hand, has drawn attention that ultracold atomic systems with graded index profiles may not necessarily have perfect transverse confinement due to simultaneously competing effects of lensing and waveguiding [8]. The experiment is based upon a recoil-induced resonance (RIR) in the high gain regime, employed for an ultracold atomic system as a graded index waveguiding medium. As a result of large core radius with high refractive index contrast, and strong dispersion due to RIR, radially confined multimode slow light propagation has been realized [8]. As also noted in the experiment, a promising and intriguing regime would have few modes where guided nonlinear optical phenomena could happen [8].

It has already been shown that the few mode regime of ultraslow waveguiding can be accessed by taking advantage of the sharp density profile of BEC and the strong dispersion provided by the usual EIT [5]. Present work aims to reconsider this result by taking into account the simultaneous lensing component. On one hand, the lensing could be imagined as a disadvantage against reliable high capacity quantum memory applications. Our investigations do aid to comprehend the conditions of efficient transverse confinement. On the other hand, we argue that because the lensing component is also strongly delayed with a time scale that can be observably large relative to the waveguiding modes, such spatially resolved slow pulse splitting can offer intriguing possibilities for creating and manipulating flying bits of

information, especially in the nonlinear regime. Indeed, earlier proposals to split ultraslow pulses in some degrees of freedom (typically polarization), face many challenges of complicated multi-level schemes, multi-EIT windows, and high external fields [9]. Quite recently birefringent lensing in atomic gaseous media in EIT setting has been discussed [10]. The proposed splitting of lensing and guiding modes is both intuitively and technically clear, and easy to implement in EIT setting, analogous to the RIR experiment.

The paper is organized as follows: After describing our model system briefly in Sec. 2, EIT scheme for an interacting BEC is presented in Sec. 3. Subsequently we focus on the lensing effect of the ultraslow pulse while reviewing already known waveguiding results shortly in Sec. 4. Main results and their discussion are in Sec. 5. Finally, we conclude in Section 6.

## 2. Model System

We consider oblique incidence of a Gaussian beam pulse onto the cigar shaped condensate as depicted in Fig. (1). Due to particular shape of the condensate two fractions, the one along the long ( $z$ ) axis of the condensate and the parallel the short ( $r$ ) axis, of the incident Gaussian beam exhibit different propagation characteristics. The  $r$ -fraction exhibit the lensing effect and focused at a focal length ( $f$ ) while the axial component would be guided in a multi mode or single mode formation.

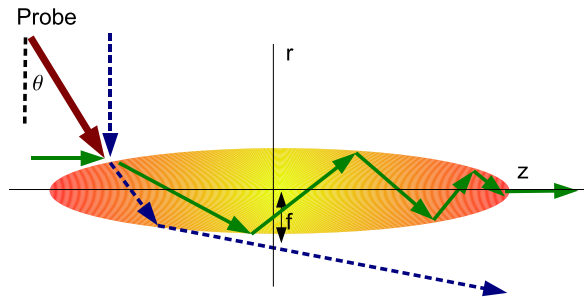


Figure 1: Lensing and waveguiding effects in a slow Gaussian beam scheme with an ultra-cold atomic system.

The angle of incidence ( $\theta$ ) controls the fraction of the probe power converted either to the lensing mode or to the guiding modes. When both lensing and waveguiding simultaneously happen in an ultraslow pulse propagation

set up, an intriguing possibility arises. Different density profiles along radial and axial directions translates to different time delays of the focused and guided modes. Due to significant difference in the optical path lengths of guided and focused components, an adjustable relative time delay can be generated between these two components. As a result, these two components become spatially separated. The fraction of the beam parallel to the short axis of the condensate undergoes propagation in a lens-like quadratic index medium resulting in a change in the spot size or the beam waist of the output beam. We call this as the lensing effect and the corresponding fraction as the lensed-fraction. The fraction of the beam propagating along the long axis is propagating in weakly-guided regime of graded index medium that can be described in terms of LP modes. This is called as guiding effect and the corresponding fraction is called as guided fraction. We use the usual Gaussian beam transformation methods under paraxial approximation to estimate the focal length. In addition our aim is to estimate time delay between these two fractions. The output lensed and guided fractions of the incident beam are delayed in time relative to each other. In general temporal splitting depends on modal, material and waveguide dispersions. For a simple estimation of relative time delay of these components, we consider only the lowest order modes in the lensed and the guided fractions, and take the optical paths as the effective lengths of the corresponding short and long axes of the condensate. In this case we ignore the small contributions of modal and waveguide dispersions and determine the group velocity, same for both fractions, by assuming a constant peak density of the condensate in the material dispersion relation.

### 3. EIT scheme for an interacting BEC

A Bose gas can be taken as condensate part and thermal part at low temperature. Following Ref. [11], density profile of BEC can be written by  $\rho(\vec{r}) = \rho_c(\vec{r}) + \rho_{\text{th}}(\vec{r})$ , where  $\rho_c(\vec{r}) = [(\mu(T) - V(\vec{r}))/U_0]\Theta(\mu - V(\vec{r}))$  is the density of the condensed atoms and  $\rho_{\text{th}}$  is the density of the thermal ideal Bose gas. Here  $U_0 = 4\pi\hbar^2 a_s/m$ ;  $m$  is atomic mass;  $a_s$  is the atomic s-wave scattering length.  $\Theta(\cdot)$  is the Heaviside step function and  $T_C$  is the critical temperature. The external trapping potential is  $V(\vec{r}) = (m/2)(\omega_r^2 r^2 + \omega_z^2 z^2)$  with trap frequencies  $\omega_r, \omega_z$  for the radial and axial directions, respectively. At temperatures below  $T_c$ , the chemical potential  $\mu$  is evaluated by  $\mu(T) = \mu_{TF}(N_0/N)^{2/5}$ , where  $\mu_{TF}$  is the chemical potential obtained under Thomas-

Fermi approximation,  $\mu_{TF} = ((\hbar\omega_t)/2)(15Na_s/a_h)^{2/5}$ , with  $\omega_t = (\omega_z\omega_r^2)^{1/3}$  and  $a_h = \sqrt{\hbar/(\omega_z\omega_r^2)^{1/3}}$ , the average harmonic oscillator length scale. The condensate fraction is given by  $N_0/N = 1 - x^3 - s\zeta(2)/\zeta(3)x^2(1 - x^3)^{2/5}$ , with  $x = T/T_c$ , and  $\zeta$  is the Riemann-Zeta function. The scaling parameter  $s$  is given by  $s = \mu_{TF}/k_B T_C = (1/2)\zeta(3)^{1/3}(15N^{1/6}a_s/a_h)^{2/5}$ .

Treating condensate in equilibrium and under Thomas-Fermi approximation (TFA) is common in ultraslow light literature and generally a good approximation because density of an ultracold atomic medium is slowly changing during the weak probe propagation. The propagation is in the order of microseconds while atomic dynamics is in millisecond time scales. Due to weak probe propagation under EIT conditions, most of the atoms remain in the lowest state[12]. The validity of TFA further depends on the length scale of the harmonic potential. If the length scale is much larger than the healing length, TFA with the harmonic potential works fine. The healing length of the BEC is defined as  $\xi = [1/(8\pi na_s)]^{1/2}$  [13] where  $n$  is the density of an atomic Bose-Einstein condensate and it can be taken as  $n = \rho(0, 0)$ . We consider range of parameters in this work within the range of validity of TFA. The interaction of atomic BEC with strong probe and the coupling pump field may drive atomic BEC out of equilibrium. This non- equilibrium discussion is beyond the scope of the present paper.

We consider, beside the probe pulse, there is a relatively strong coupling field interacting with the condensate atoms in a  $\Lambda$ -type three level scheme with Rabi frequency  $\Omega_c$ . The upper level is coupled to the each level of the lower doublet either by probe or coupling field transitions. Under the weak probe condition, susceptibility  $\chi$  for the probe transition can be calculated as a linear response as most of the atoms remain in the lowest state. Assuming local density approximation, neglecting local field, multiple scattering and quantum corrections and employing steady state analysis we find the well-known EIT susceptibility [1, 14],  $\chi_i, i = r, z$ , for either radial ( $r$ ) or axial ( $z$ ) fraction of the probe pulse. Total EIT susceptibility for BEC in terms of the density  $\rho$  can be expressed as  $\chi_i = \rho_i \chi_1$  in the framework of local density approximation. Here  $\chi_1$  is the single atom response given by

$$\chi_1 = \frac{|\mu|^2}{\varepsilon_0 \hbar} \frac{i(-i\Delta + \Gamma_2/2)}{(\Gamma_2/2 - i\Delta)(\Gamma_3/2 - i\Delta) + \Omega_C^2/4}, \quad (1)$$

where  $\Delta$  is the detuning from the resonant probe transition . For the ultra-cold atoms and assuming co-propagating laser beams, Doppler shift in the

detuning is neglected.  $\mu$  is the dipole matrix element for the probe transition. It can also be expressed in terms of resonant wavelength  $\lambda$  of the probe transition via  $\mu = 3\varepsilon_0\hbar\lambda^2\gamma/8\pi^2$ , where  $\gamma$  is the radiation decay rate of the upper level.  $\Gamma_2$  and  $\Gamma_3$  denote the dephasing rates of the atomic coherences of the lower doublet. At the probe resonance, imaginary part of  $\chi$  becomes negligible and results in turning an optically opaque medium transparent.

## 4. Propagation of beam through a quadratic index medium

### 4.1. Lensing effect

We can neglect thermal part of a Bose gas due to the high index contrast between the condensate and the thermal gas background so that  $\rho = \rho_c$ . We specifically consider a gas of  $N = 8 \times 10^6$   $^{23}\text{Na}$  atoms with  $\Gamma_3 = 0.5\gamma$ ,  $\gamma = 2\pi \times 10^7\text{Hz}$ ,  $\Gamma_2 = 7 \times 10^3\text{ Hz}$ , and  $\Omega_c = 2\gamma$ . We take  $\omega_r = 160\text{ Hz}$  and  $\omega_z = 40\text{ Hz}$ . For these parameters, we evaluate  $\chi' = 0.02$  and  $\chi'' = 0.0004$  at  $\Delta = 0.1\gamma$ , where  $\chi'$  and  $\chi''$  are the real and imaginary parts of  $\chi$ , respectively. Neglecting  $\chi''$ , the refractive index becomes  $n = \sqrt{1 + \chi'}$ . In the  $z$  direction it can be written as [15, 16]

$$n(z) = n_0[1 - \beta_z^2 z^2]^{1/2}, \quad (2)$$

where  $n_0 = (1 + \mu\chi'_1/U_0)^{1/2}$  and quadratic index coefficient is  $\beta_z^2 = \chi'_1 m \omega_z^2 / (2U_0 n_0^2)$ . Thomas-Fermi radius for the axial coordinate is given by  $R_{TF_z} = \sqrt{2\mu(T)/m\omega_z^2}$ . Expanding Eq. (2) in Taylor series, the refractive index reduces to

$$n(z) \approx n_0[1 - \frac{1}{2}\beta_z^2 z^2]. \quad (3)$$

The refractive index as a function of  $z$  is shown in Fig. 2. With such a refractive index profile, the atomic medium can act as a thin lens for the component of the probe in the radial direction. In the case of a medium with a quadratic index variation, we can estimate the focal length by using geometrical or beam optics [15, 16]. In the paraxial geometrical optics regime, where the angle made by the beam ray with optic axis is small, the differential equation satisfied by the ray height  $s(r)$  is  $d^2s/dr^2 + \beta_z^2 r = 0$  [15, 16]. The initial ray height and initial slope are  $r_i$ ,  $\theta_i = ds/dr|_i$  respectively. The solutions of the differential equation are  $s(r) = r_i \cos(\beta_z r) + 1/\beta_z \sin(\beta_z r)\theta_i$

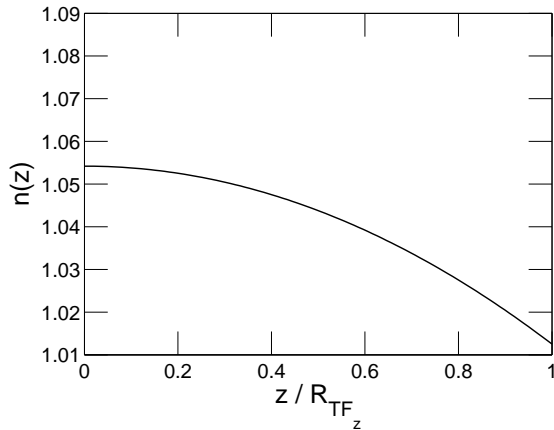


Figure 2:  $z$  dependence of the refractive index of a condensate of  $8 \times 10^6$   $^{23}$  Na atoms at  $T = 296$  nK under off-resonant EIT scheme. The other parameters used are  $\Omega_c = 1.5 \times \gamma$ ,  $\Delta = 0.1 \times \gamma$ ,  $M = 23$  amu,  $\lambda_0 = 589$  nm,  $\gamma = 2\pi \times 10^7$  Hz,  $\Gamma_3 = 0.5\gamma$ ,  $\Gamma_2 = 7 \times 10^3$  Hz.

and  $\theta(z) = ds/dr = -\beta_z \sin(\beta_z r)r_i + \cos(\beta_z r)\theta_i$ . Hence, the ray transformation matrix  $M_T$  which connects the initial and final ray vectors is given by Eq. (4), where  $r$  is the propagation length in the medium. [15, 16, 17]

$$M_T = \begin{pmatrix} \cos(\beta_z r) & \frac{1}{\beta_z} \sin(\beta_z r) \\ -\beta_z \sin(\beta_z r) & \cos(\beta_z r) \end{pmatrix}. \quad (4)$$

The same ray transformation matrix given by Eq. (4) can be used to investigate the effect of the quadratic medium on the light in the beam optics regime. Consider a collimated Gaussian beam incident on a focusing ultra cold medium represented by  $M_T$ . The  $q$  parameter  $q(r)$  of the Gaussian beam which describes the spot size and the radius of curvature of the beam is given by

$$\frac{1}{q(r)} = \frac{1}{R(r)} - i \frac{\lambda}{n\pi w(r)^2}, \quad (5)$$

where  $w(r)$  is the spot-size function, and  $n$  is the medium refractive index. If the incident beam is collimated,  $R(r) \rightarrow \infty$ , and the initial  $q$ -parameter  $q_1$  becomes  $iz_0$ , where the Rayleigh range  $z_0$  is given by  $z_0 = \pi\omega_0^2/\lambda$ . Here,  $\omega_0$  is the initial beam waist on the BEC and we assumed that the background refractive index is nearly 1. After a distance of  $r$  inside the BEC, the

transformed  $q$ -parameter  $q_2$  will given by

$$q_2 = \frac{iz_0 \cos(\beta_r r) + \frac{1}{\beta_z} \sin(\beta_z r)}{-iz_0 \beta_z \sin(\beta_z r) + \cos(\beta_z r)}. \quad (6)$$

We have two cases to consider for focusing. If the BEC is very thin, the focal length will be approximately given by  $1/\beta_z^2 L_r$  where  $L_r$  is the transverse width of the BEC. If the BEC length is not negligible, the next collimated beam will be formed inside the BEC at the location  $L_f$ , given by  $\beta_z L_f = \pi/2$ .

#### 4.2. Waveguiding effect

Along the radial direction, similar to previous treatment, refractive index profile in the radial direction can be written as

$$n(r) = \begin{cases} n_0 [1 - \frac{1}{2} \beta_r^2 r^2]^{1/2} & r \leq R_{TFr} \\ 1 & r \geq R_{TFr} \end{cases}, \quad (7)$$

where  $n_0 = (1 + \mu \chi'_i / U_0)^{1/2}$  and  $\beta_r^2 = \chi'_1 m \omega_z^2 / (2U_0 n_0^2)$ . Thomas-Fermi radius is given by  $R_{TFr} = \sqrt{2\mu(T)/m\omega_r^2}$ .

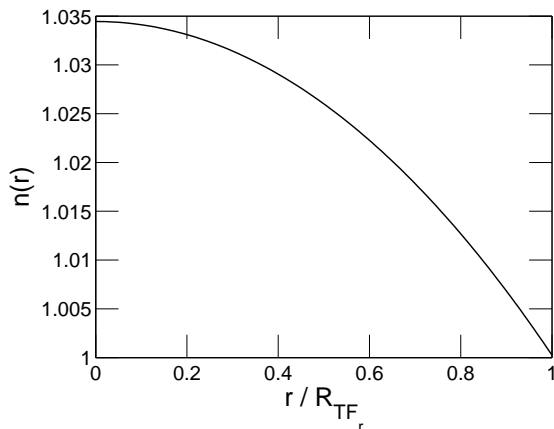


Figure 3:  $r$  dependence of the refractive index of the condensate. The parameters are the same as Fig. (2)

The refractive index which is given in Eq.(7) is plotted as a function of  $r$  in Fig.3. Expanding Eq. (7) in Taylor series, the refractive index reduces to



$n(r) \approx n_0(1 - 0.5\beta_r^2 r^2)$ . Such an index behavior is analogous to the one of a graded index fiber [5]. Slow light propagation through the condensate can be described similar to that of the weakly guided regime of the graded index fiber, where the optical modes can be given in terms of linearly polarized modes (LP modes). The mode profiles are determined by solving the wave equation which reduces to the Helmholtz equation [5].

We use the cylindrical coordinates as the refractive index  $n(r)$  is axially symmetric. The wave equation for the axial fraction of the probe field is  $[\nabla^2 + k^2]E = 0$ , where  $k^2 = k_z^2 + k_r^2$  and  $\nabla^2$  is the Laplacian operator in cylindrical coordinate. Here  $k_r$  is the radial wave number and  $k_z$  is the propagation constant in the  $z$  direction. The solution for the wave equation is  $E = \psi(r) \cos(l\phi) \exp[i(\omega t - k_z z)]$ . Here  $l = 0, 1, 2, 3, \dots$  and  $\phi$  is the absolute phase. If we put this solution in the wave equation, we get the Helmholtz radial equation

$$[d^2/dr^2 + (1/r)d/dr + p^2(r)]\psi(r) = 0, \quad (8)$$

in which  $p^2(r) = (k_0^2 n^2(r) - k_z^2 - l^2/r^2)$  [15]. Here  $k_0$  can be expressed in terms of resonant wavelength  $\lambda$  of the probe transition  $k_0 = 2\pi/\lambda = 1.07 \times 10^7$  (1/m).

We use transfer matrix method developed in Ref. [5] in order to solve the Helmholtz equation. Eq.(8).

We assume that the atomic cloud can be described by layers of constant refractive index, such that, their indices monotonically increase towards the center of the cloud. By taking sufficiently large number of thin layers such a discrete model can represent the true behavior of the refractive index. For constant index, analytical solutions of the Helmholtz equation can be found in terms of Bessel functions. Such solutions are then matched at the shell boundaries of the layers. Doing this for all the layers, electromagnetic boundary conditions provide a recurrence relation for the Bessel function coefficients, whose solution yields the wave number  $k$ . The mode profiles determined by this method are shown in Fig. (6), and Fig. (7).

## 5. Results and Discussions

### 5.1. Lensing Properties

The condensate can act as a lens or a guiding medium depending on the Rayleigh range of the probe relative to the effective length of the condensate

[8]. For the cigar shaped BEC geometry we consider, the radial fraction of the probe is subject to lensing while the axial fraction is guided. Let us first examine the focal length of the condensate for the radial fraction of the incident probe. For that aim we need to determine the effective radial length

$$L_r = \left[ \int_V d^3r r^2 \rho(r, z) \right]^{1/2}, \quad (9)$$

corresponding to the radial rms width of the density distribution. Radial component of the probe field enters the medium and converges at a focus distance, determined

$$f = \frac{1}{\beta_z^2 L_r}. \quad (10)$$

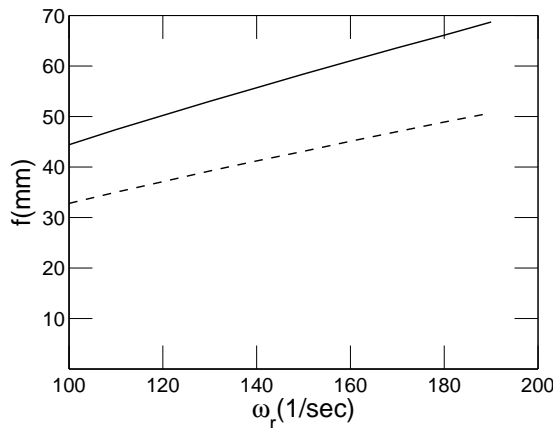


Figure 4: Behavior of the focus length with respect to trap frequency for the radial direction and scattering length. The solid curve is for  $a_s = 5$  nm and the dashed curve is for  $a_s = 7$  nm. The other parameters are the same as Fig. (2)

Focal length is plotted in as shown in Fig. (4) as a function of trap frequency for the radial direction and with the scattering length at a temperature  $T = 296$  nK. The increase in the radial trap frequency leads to decrease in the radial size of the BEC, which causes the rise of the focal length seen in Fig. (4). In contrast, the size of the condensate increases by atom-atom interactions, characterized by the scattering length  $a_s$ , which causes an overall reduction of the focal length.

## 5.2. Waveguiding Properties

For the cigar shaped BEC geometry we consider again the axial fraction of the probe is subject to guided. The effective axial length is determined by

$$L_z = \left[ \frac{4\pi}{N} \int_0^\infty r dr \int_0^\infty dz z^2 \rho(r, z) \right]^{1/2}. \quad (11)$$

The axial length  $L_z$  is an effective length corresponding to the axial width of the density distribution. Group velocities ( $v_{gi}, i = r, z$ ) of the different density profiles for both radial and axial directions can be calculated from the susceptibility using the relations

$$\frac{1}{v_{gi}} = \frac{1}{c} + \frac{\pi}{\lambda} \frac{\partial \chi_i}{\partial \Delta}. \quad (12)$$

Here,  $c$  is the speed of light and imaginary part of the susceptibility is negligibly small relative to the real part of it. EIT can be used to achieve ultraslow light velocities, owing to the steep dispersion of the EIT susceptibility  $\chi$  [3]. In general temporal splitting depends on modal, material and waveguide dispersions. For a simple estimation of relative time delay of these components, we consider only the lowest order modes in the lensed and the guided fractions, and take the optical paths as the effective lengths of the corresponding short and long axes of the condensate. In this case we ignore the small contributions of modal and waveguide dispersions and determine the group velocity, same for both fractions, by assuming a constant peak density of the condensate in the material dispersion relation. Density profiles along radial and axial directions lead to different time delays of the focused and guided modes. Due to significant difference in the optical path lengths of guided and focused components, a certain time delay can be generated between these two components.

Taking into account transverse confinement, ultraslow Gaussian beam propagation along the long axis of a BEC can be described in terms of multiple LP modes, propagating at different ultraslow speeds [5]. In the geometry and system we consider here, for instance, there can be found approximately 44 modes at temperature  $T = 42$  nK. We compare the delay time of the slowest mode (the lowest guided mode) with that of the lensing mode which can be respectively calculated by  $t_{Dz} = L_z/v_{gz}$  and  $t_{Dr} = L_r/v_{gr}$ . Thermal behaviors of the time delays are shown in Fig. (5). Fig. (5) indicates that due to different refractive indices seen by the axial and radial fractions of the

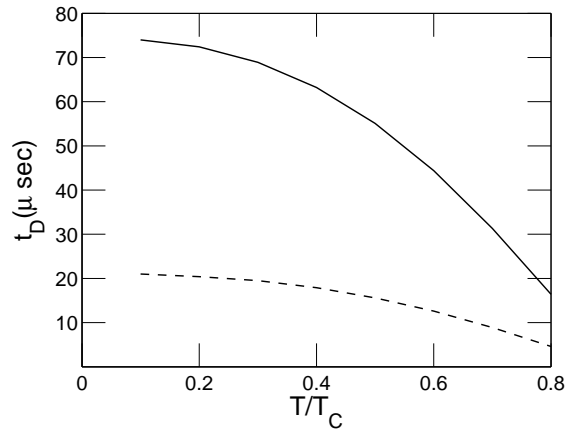


Figure 5: Thermal behavior of the time delays of the guided and focused fractions. The solid and dashed lines are for  $t_{Dz}$  and  $t_{Dr}$ , respectively. The parameters are the same as Fig. (2) except  $\Omega_c = 0.5\gamma$

probe, significant temporal delay,  $\sim 50 \mu\text{s}$ , can occur between them at low temperatures  $T \sim 42 \text{ nK}$ . Time delays for each fraction decreases with the temperature. Besides, the relative difference of their time delays diminishes with the temperature. The condensed cloud shrinks due to the increase in temperature, so that effective lengths of the BEC diminish. Therefore, just below  $T_C$ , time delays drop to zero.

At low temperatures waveguiding modes can occur in an atomic Bose-Einstein condensate because of an atomic Bose-Einstein condensate. Translation of the Thomas-Fermi density profile of the condensate to the refractive index makes the medium gain waveguiding characteristics analogous to those of a graded index fiber [5, 8]. For the same set of parameters, for which the radial fraction of the probe undergoes lensing effect, the axial fraction is guided in multiple LP modes, as the corresponding Rayleigh range is larger than the effective axial length. The lowest two LP modes are shown in Fig. (6), and Fig. (7). The total number of modes that can be supported by the condensate is determined by the dimensionless normalized frequency  $V$  which is defined as  $V = (\omega/c)R(n_0^2 - 1)^{1/2}$  where  $R = \sqrt{2\mu(T)/m\omega_r^2}$  [5]. The radius of a condensate that would support only single mode,  $\text{LP}_{00}$ , is found to be  $R \sim 1 \mu\text{m}$ . In principle this suggest that simultaneous lensing and single LP mode guiding should also be possible.

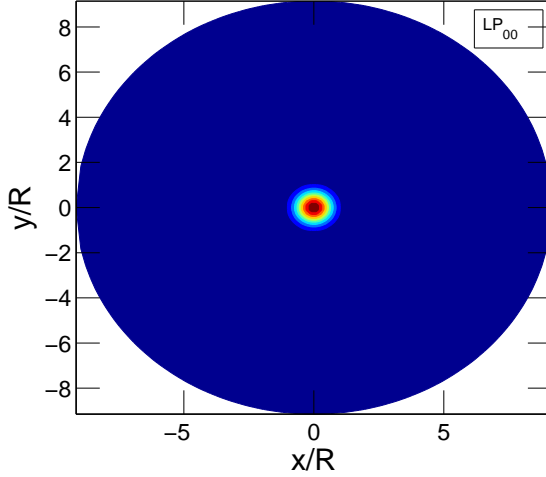


Figure 6: Contour plot of intensity of the  $\psi_{00} \exp[i(\omega t - \beta_z z)]$  ( $LP_{00}$  mode). The parameters are the same as Fig. (5)

## 6. Conclusion

We investigate simultaneous lensing and ultraslow waveguiding properties of atomic condensate under EIT conditions by using a quadratic-index model of the medium. The focus length, relative time delay, and multiple guided mode characteristics are determined taking into account three dimensional nature of the system. In particular, dependence of focus length on atom-atom interactions via s-wave scattering length, and on trap frequency and temperature are examined. Our results reveal how to select a suitable set of system parameters to tune Rayleigh range and the aspect ratio of the cloud to make either lensing or guiding more favorable along a particular direction. We have shown that the focus length can be calibrated by the transverse trap frequency, incoming wave length, scattering length and temperature. In addition, time-delayed splitting of ultraslow Gaussian beam into radial and axial fractions is found.

## Acknowledgements

We thank Z. Dutton for valuable and useful discussions. D.T. was supported by TUBITAK-Kariyer grant No. 109T686. Ö.E.M. acknowledges

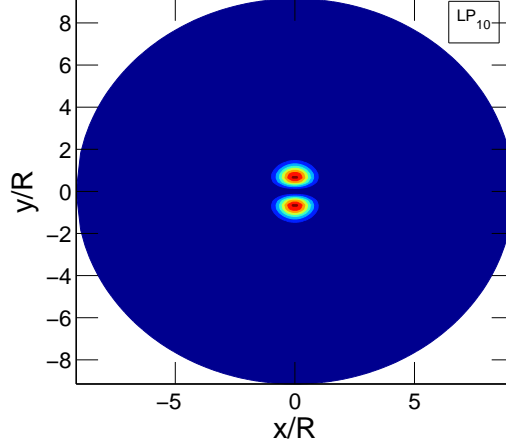


Figure 7: Contour plot of intensity of the  $\psi_{10} \cos(\phi) \exp[i(\omega t - \beta_z z)]$  (LP<sub>10</sub> mode). The parameters are the same as Fig. 5.

support by TUBITAK (109T267) and DPT-UEKAE quantum cryptology center.

## References

- [1] S.E. Harris, *Physics Today* 50 (1997) 36-42.
- [2] M. Fleischhauer, A. Imamoglu, and J. P. Marangos, *Rev. Mod. Phys.* 77 (2005) 633.
- [3] L.V. Hau, S.E. Harris, Z. Dutton, C.H. Behroozi, *Nature* 397 (1999) 594-598.
- [4] J. Cheng, S. Han, Y. Yan, *Phys. Rev. A* 72 (2005) 021801(R).
- [5] D. Tarhan, N. Postacioglu, Ö. E. Müstecaplıođlu, *Opt. Lett.* 32 (2007) 1038.
- [6] F. L. Kien, and K. Hakuta, *Phys. Rev. A* 79 (2009) 043813.
- [7] G. Morigi, and G. S. Agarwal, *Phys. Rev. A* 79 (2000) 013801.

- [8] M. Vengalattore, and M. Prentiss, Phys. Rev. Lett. 95 (2005) 243601.
- [9] G. S. Agarwal, and S. Dasgupta, Phys. Rev. A 65 (2002) 053811.
- [10] H. R. Zhang, L. Zhou and C. P. Sun, Phys. Rev. A 80 (2009) 013812.
- [11] M. Naraschewski, D.M. Stamper-Kurn, Phys. Rev. A 58 (1998) 2423.
- [12] Z. Dutton, and L. V. Hau, Phys. Rev. A 70 (2004) 053831.
- [13] C. J. Pethick and H. Smith, Bose-Einstein Condensation in Dilute Gases, Cambridge, Cambridge, 2002.
- [14] M.O. Scully, M.S. Zubairy, Quantum Optics, Cambridge, Cambridge, 1997.
- [15] A. Yariv, Optical Electronics, Saunders College, Holt, Rinehart and Winston, 1991.
- [16] A. Sennaroglu, Photonics and Laser Engineering: Principles, Devices and Applications, New York, McGraw-Hill, 2010.
- [17] L. Casperson, A. Yariv, Appl. Phys. Lett. 12 (1968) 355.